CORRECTION

Correction: Adaptive signatures in thermal performance of the temperate coral *Astrangia poculata*

Hannah E. Aichelman, Richard C. Zimmerman and Daniel J. Barshis

There was an error in *J. Exp. Biol.* (2019) **222**, jeb189225 (doi:10.1242/jeb.189225).

It was reported that no permits were required for collection of the Rhode Island corals used in the study. This was an error, and the necessary permits were in place for all coral collections. Both the online full text and PDF versions of the paper have been corrected. The authors apologise to the readers for this error.

The Company of
Biologists

RESEARCH ARTICLE

Adaptive signatures in thermal performance of the temperate coral *Astrangia poculata*

Hannah E. Aichelman[1,*], Richard C. Zimmerman[2] and Daniel J. Barshis[1]

ABSTRACT

Variation in environmental characteristics and divergent selection pressures can drive adaptive differentiation across a species' range. *Astrangia poculata* is a temperate scleractinian coral that provides unique opportunities to understand the roles of phenotypic plasticity and evolutionary adaptation in coral physiological tolerance limits. This species inhabits hard-bottom ecosystems from the northwestern Atlantic to the Gulf of Mexico and withstands an annual temperature range of up to 20°C. Additionally, *A. poculata* is facultatively symbiotic and co-occurs in both symbiotic ('brown') and aposymbiotic ('white') states. Here, brown and white *A. poculata* were collected from Virginia (VA) and Rhode Island (RI), USA, and exposed to heat (18–32°C) and cold (18–6°C) stress, during which respiration of the coral host along with photosynthesis and photochemical efficiency (F_v/F_m) of *Breviolum psygmophilum* photosymbionts were measured. Thermal performance curves (TPCs) of respiration revealed a pattern of countergradient variation with RI corals exhibiting higher respiration rates overall, and specifically at 6, 15, 18, 22 and 26°C. Additionally, thermal optimum (T_{opt}) analyses show a 3.8°C (brown) and 6.9°C (white) higher T_{opt} in the VA population, corresponding to the warmer *in situ* thermal environment in VA. In contrast to respiration, no origin effect was detected in photosynthesis rates or F_v/F_m, suggesting a possible host-only signature of adaptation. This study is the first to consider *A. poculata*'s response to both heat and cold stress across symbiotic states and geography, and provides insight into the potential evolutionary mechanisms behind the success of this species along the East Coast of the USA.

KEY WORDS: Facultative symbiosis, Thermal performance curve, Local adaptation, Countergradient variation, G matrix, Mitochondrial proliferation

INTRODUCTION

Environmentally driven population differentiation represents an equilibrium between divergent selection pressures and the homogenizing effects of gene flow (e.g. García-Ramos and Kirkpatrick, 1997; Hendry et al., 2002; Kawecki and Ebert, 2004; Sanford and Kelly, 2011). Historically, gene flow was thought to be high in the marine environment owing to the misconception that marine populations were well mixed as a result of high connectivity, limited barriers to dispersal, and the prevalence of planktonic larval

stages (Palumbi, 2004; Sanford and Kelly, 2011). However, several recent studies on marine invertebrates have demonstrated population differentiation consistent with adaptation at a variety of spatial scales. For example, signatures of adaptation to local thermal environments were observed in corals in American Samoa among populations separated by <1 km (Barshis et al., 2018, 2010; Bay and Palumbi, 2014; Palumbi et al., 2014) and between populations of corals in the Florida Keys separated by <10 km (Kenkel et al., 2013). Additionally, signatures of adaptive differentiation (i.e. differences in thermal tolerance with latitude) were observed in green crabs across both the native European range and the invasive US East Coast range (Tepolt and Somero, 2014). A difference in local (for corals) or native (for green crabs) thermal environments was postulated as the environmental driver behind the evolution of adaptive differentiation among contrasting habitat types.

Temperature is fundamental to the chemistry of life (Arrhenius, 1889). It plays a major role in shaping an organism's growth, survival, reproduction and population density, as well as species distributions and patterns of species diversity (Angilletta, 2009; Hochachka and Somero, 2002; Schulte et al., 2011). Adaptation to distinct thermal environments along a species' range could therefore result in differential responses or susceptibility to temperature variation throughout that range. These population-level responses to environmental variability and thermal conditions are of particular concern in an era of climate change. Understanding the mechanisms by which temperature affects populations and their distribution will assist in predicting the 'winners' and 'losers' under future conditions (Loya et al., 2001; Somero, 2010; van Woesik et al., 2011) and will help to estimate the adaptive genetic variation present in metapopulations that could power rapid adaptation to climate change (i.e. Bay et al., 2017; Kleypas et al., 2016; Matz et al., 2018).

Thermal performance curves (TPCs) are often used to quantify the effect of temperature on organismal performance within a particular zone of tolerance (Angilletta, 2009; Huey and Stevenson, 1979; Schulte et al., 2011). TPCs tend to exhibit the same general shape, in which performance increases with temperature to some thermal optimum (T_{opt}) and then rapidly decreases (Angilletta et al., 2002; Angilletta, 2009; Huey and Kingsolver, 1989; Huey and Kingsolver, 1993; Huey and Stevenson, 1979). TPCs have been used previously to understand the response of different populations to increasing temperatures (e.g. Gardiner et al., 2010) and to predict organism responses to climate change (e.g. Schulte et al., 2011). When comparing TPCs from multiple populations of the same species across a thermal gradient, several patterns might be expected (Angilletta, 2009; Gardiner et al., 2010). First, thermal optima could be adapted to the local thermal environment, meaning that populations from warmer sites will display an elevated phenotype (i.e. elevated performance, depending on the phenotype measured) compared with populations from cooler sites at warmer temperatures, and vice versa (Angilletta, 2009). Second, populations from warmer

[1]Department of Biological Sciences, Old Dominion University, 110 Mills Godwin Life Sciences Building, Norfolk, VA 23529, USA. [2]Department of Ocean, Earth, and Atmospheric Sciences, Old Dominion University, 4600 Elkhorn Avenue, Norfolk, VA 23529, USA.

*Author for correspondence (hannahaichelman@gmail.com)

H.E.A., 0000-0001-6999-5518

List of symbols and abbreviations

F_v/F_m	symbiont photochemical efficiency
ODU	Old Dominion University
OTU	operational taxonomic unit
P	photosynthesis
P_{corr}	gross photosynthesis corrected for rates of commensals (μmol O_2 cm^2 h^{-1})
P_{gross}	gross photosynthesis (μmol O_2 cm^2 h^{-1})
P_{max}	maximum rate of photosynthesis (μmol O_2 l^{-1} min^{-1})
P_{net}	net photosynthesis (μmol O_2 cm^2 h^{-1})
R	respiration
R_{corr}	dark respiration corrected for rates of commensals (μmol O_2 cm^2 h^{-1})
RI	Rhode Island
SST	sea surface temperature (°C)
T_{opt}	thermal optimum
TPC	thermal performance curve
VA	Virginia

sites could display an elevated phenotype compared with populations from colder sites at all temperatures (evidence of cogradient variation; Conover et al., 2009). Third, populations from cold sites could display an elevated phenotype compared with populations from warm sites at all temperatures (evidence of countergradient variation; Angilletta, 2009). Finally, there could be no difference in phenotype between populations (Angilletta, 2009; Gardiner et al., 2010). It is imperative to understand how temperature affects different populations when predicting how a species may respond to future environmental change at large spatial scales (Gardiner et al., 2010; Schulte et al., 2011).

The northern star coral, *Astrangia poculata* (=*A. danae*; Ellis & Solander 1786; Peters et al., 1988), is a temperate scleractinian coral that has two primary characteristics that distinguish it from tropical scleractinians and make it a particularly interesting species for studying coral thermal physiology. First, *A. poculata* is facultatively symbiotic and exists both in symbiosis with endosymbiotic algae of the family Symbiodiniaceae (symbiotic, or brown), specifically *Breviolum psygmophilum* (LaJeunesse et al., 2012), as well as without this symbiosis (aposymbiotic, or white). This facultative symbiosis is quite different from the obligate symbiosis common to the majority of tropical scleractinians. Additionally, it enables independent characterizations of the relative role that coral hosts and *B. psygmophilum* play in thermal tolerance, as the response of the host can be isolated in experiments using aposymbiotic colonies. Second, *A. poculata* has an extensive range, inhabiting hard-bottom environments from the Gulf of Mexico to Cape Cod, Massachusetts (Peters et al., 1988; Thornhill et al., 2008), spanning a wide range of environmental conditions, particularly temperature, both within and among sites. For example, in Rhode Island, *A. poculata* thrives in temperatures that reach 27°C in the summer and drop to as low as 0°C in the winter (Dimond and Carrington, 2007). This characteristic is drastically different from tropical corals, which are generally limited to a narrow thermal range of less than 10°C (Veron, 2000). The majority of previous studies on *A. poculata* have focused on sites from the northern end of this species' range, including Rhode Island (e.g. Burmester et al., 2017; DeFilippo et al., 2016; Dimond and Carrington, 2007; Jacques et al., 1983; Jacques and Pilson, 1980) and Massachusetts (e.g. Holcomb et al., 2012, 2010; Ries, 2011). Although some Mid-Atlantic shipwrecks are extensively covered by *A. poculata* (up to 75%, H.E.A. and D.J.B., personal observation),

there is very little known about this species in the more central and southern parts of its range, which experience higher temperatures.
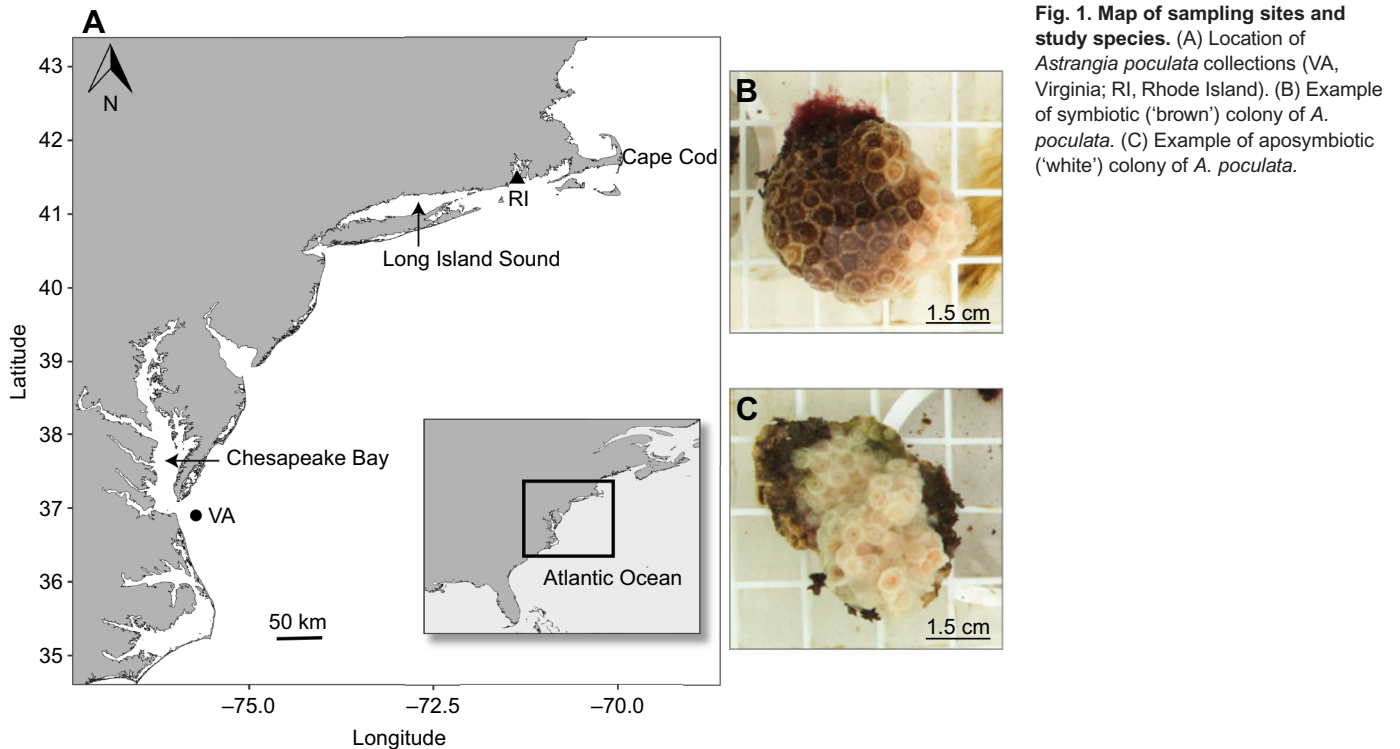
Here, we conducted a common garden experiment to look for phenotypic evidence of adaptation in thermal performance of the temperate coral *A. poculata*. The goal was to investigate whether thermal performance of *A. poculata* differed across unique thermal environments or by symbiotic status. We measured metabolic rates [respiration (R) and photosynthesis (P)] of brown and white *A. poculata* as well as the dark-adapted quantum yield of photochemistry in photosystem II (PSII), hereafter referred to as photochemical efficiency (F_v/F_m; reviewed by Fitt et al., 2001), at a range of temperatures (6 to 32°C) from two sites along the species' range [Virginia (VA) and Rhode Island (RI); Fig. 1]. Because sea surface temperatures (SST) in VA are consistently warmer over the course of the year (Fig. 2A), we hypothesized that VA corals would be adapted to warmer temperatures, and therefore exhibit a higher T_{opt} compared with RI corals (the first scenario outlined above). All of the traits measured here were also used to create a genetic variance–covariance matrix (**G** matrix) to investigate whether adaptive signatures between the two populations involve changes in the genetic architecture of traits. This work assesses the potential for adaptation of coral physiology to environmental conditions at a regional spatial scale and has implications for understanding how *A. poculata* in the temperate northwest Atlantic could respond to future temperature increases associated with climate change, particularly in light of the fact that recent warming has been more pronounced in the North Atlantic than other ocean basins (Rhein et al., 2013).

MATERIALS AND METHODS
Coral collection and transportation
In May and June 2017, 10 brown and 10 white *Astrangia poculata* colonies were collected each from VA and RI, USA (Fig. 1). VA colonies were collected from the wreck of the J. B. Eskridge (37.8992°N, 75.7225°W) on 26 May and 2 June 2017 at 20 m depth. All VA colonies were transported to the Old Dominion University (ODU) Aquatics Facility and placed in a common garden aquarium within 6 h of collection. RI colonies were collected from Fort Wetherill State Park (41.4774°N, 71.3600°W) on 9 June 2017 from a depth of approximately 11 m. RI colonies were maintained overnight at the Roger Williams University Aquatics Facility in a recirculating seawater aquarium [temperature=18°C, salinity=35 (PSS-78; Lewis, 1980)] and then transported by car in an aerated aquarium to ODU the next day. All VA and RI colonies were collected by SCUBA divers using a hammer and chisel and were separated by at least 0.5 m to ensure the collection of distinct individuals. VA corals were collected under Virginia Marine Resources Commission permit 17-017. RI corals were collected under Rhode Island Department of Environmental Management collector's permit #2017-03E.

In situ temperature environment
VA *in situ* temperature was recorded every 15 min between 23 August and 19 October 2016 and again between 6 January and 14 September 2017 using Hobo Pendant® Temperature Data Loggers (Onset Computer Corporation, Bourne, MA, USA) deployed on the wreck of the J. B. Eskridge (Fig. 2A). RI *in situ* temperature was recorded every 15 or 16 min by StowAway TidbiT Temperature Data Loggers (Onset Computer Corporation) between 11 August 2016 and 7 November 2017 deployed at the collection site (RI data courtesy of Dr Sean Grace, Southern Connecticut State University). *In situ* temperature was compared with SST recorded by the NOAA data buoys closest to the collection sites (NOAA National Data

Fig. 1. Map of sampling sites and study species. (A) Location of *Astrangia poculata* collections (VA, Virginia; RI, Rhode Island). (B) Example of symbiotic ('brown') colony of *A. poculata.* (C) Example of aposymbiotic ('white') colony of *A. poculata.*
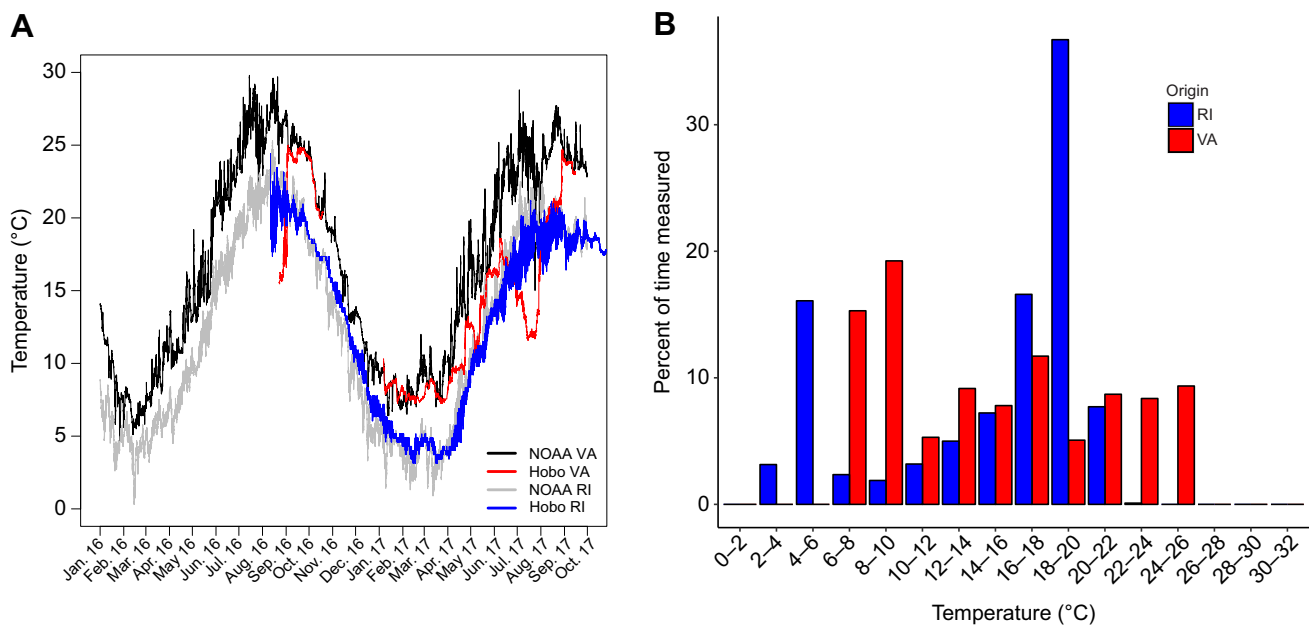
Buoy Center; Fig. 2A). VA SST data were extracted from the Cape Henry buoy (Station 44099, 36.9153°N, 75.7200°W), and RI SST data were extracted from the Newport, Rhode Island, buoy (Station 8452660, 41.5044°N, 71.3261°W).

Coral recovery and acclimation

Upon arrival at the ODU Aquatics Facility, all VA and RI individuals were placed in a common garden aquarium and

maintained at 15°C (approximate temperature at time of collection for both sites) and salinity of 35. Whole colonies were allowed to acclimate at those conditions for at least 10 days before being fragmented over 3 days (19–21 June 2017) using a high-speed cut-off tool (Chicago Pneumatic, Rock Hill, SC, USA) fitted with a diamond tip circular blade. Colony fragments were then affixed to circular stands using InstaCure ethyl cyanoacrylate gel (IC-Gel, Bob Smith Industries Inc., Atascadero, CA, USA) and returned to the

Fig. 2. Comparison of VA and RI thermal environments. (A) Sea surface temperature (SST) and temperature at collection depth of VA and RI sites between January 2016 and October 2017. SST of VA and RI sites was extracted from the Cape Henry, VA (station 44099), and Newport, RI (station 8452660), NOAA data buoys (black and gray lines, respectively). Temperature at the collection depths of the VA and RI sites (red and blue lines, respectively) was recorded by Hobo Pendant temperature loggers. (B) Percent of time that each site (VA and RI) spent at 2°C intervals between 0 and 32°C. The histogram includes Hobo Pendant logger data represented by the blue and red lines in A, excluding days where temperature was measured at only one site.

common garden aquarium. As many non-coral organisms as possible (i.e. algae, sponge and other coral-associated organisms) were removed from the coral pieces during the fragmentation process using the same high-speed cut-off tool and diamond tip circular blade.

After fragmenting, all corals were allowed to recover at 15°C for at least 1 week, after which temperature was increased by 1°C day^{-1} until the target 18°C was achieved. Coral fragments were then acclimated to the new ambient conditions for another week before respirometry experiments began (16 days recovery/acclimation post-fragmentation, at least 24 days total recovery/acclimation). The ambient temperature of 18°C was chosen for these experiments as it is a moderate temperature within the natural thermal range of both populations (Fig. 2) and has been previously reported in the literature as a control temperature for RI *A. poculata* (e.g. Burmester et al., 2017).

Experimental design
A series of 16 distinct ramp experiments were performed to determine the TPCs of photosynthesis (P), respiration (R) and *B. psygmophilum* photochemical efficiency (F_v/F_m) of VA and RI populations of *A. poculata* (Fig. S1). The 16 experiments consisted of four categories of ramp experiments: a heat ramp of the coral holobiont (18 to 32°C), a cold ramp of the coral holobiont (18 to 6°C), a heat ramp of the coral skeleton only (18 to 32°C) and a cold ramp of the coral skeleton only (18 to 6°C). Following Jacques et al. (1983), metabolic rates of the commensal organisms housed in the skeleton were measured after removing the coral tissue with an airbrush. These skeleton-only metabolic rates were subtracted from the holobiont metabolic rates to obtain corrected measures (R_{corr} and P_{corr}) of the coral host+*B. psygmophilum* metabolism. Each ramp experiment included eight unique *A. poculata* individuals (i.e. genets), including two VA-brown, two VA-white, two RI-brown and two RI-white fragments. When possible, the *A. poculata* individuals used in these experiments were cut into four fragments, allowing all genets to be represented in all four ramp categories. Thus, fragments used in the coral skeleton ramps were never subjected to a previous ramp experiment before the tissue was removed. Because of their smaller size, it was difficult to cut every RI coral colony into four fragments of sufficient size. Therefore, a total of 10 RI-brown individuals and nine RI-white individuals were used in these experiments. The four categories of ramp experiments were each repeated four times, for a total of 16 thermal performance ramps, all of which took place within 20 days of each other in July 2017.

Each of the 16 ramp experiments proceeded as follows. At approximately 07:30 h, eight experimental coral fragments were moved from the common garden aquarium to the experimental aquarium and randomly assigned to one of nine respirometry chambers. Before transferring, temperature and salinity of both the common garden and experimental aquaria were measured to ensure these parameters were equivalent (18±0.2°C and 35 salinity). Following at least a 30-min dark acclimation, oxygen consumption in the dark was recorded for 20 min to estimate dark respiration (R). Next, each chamber was flushed with non-chamber water and F_v/F_m was measured in triplicate for each fragment. Following the F_v/F_m measurements, chambers were re-sealed and oxygen evolution in the light [400 µmol photons m^{-2} s^{-1}, supplied by a single 165 W LED aquarium light (GalaxyHydro, Roleadro, Shenzhen, China) and measured using an LI-193 Spherical Underwater Quantum PAR Sensor (LI-COR, Lincoln, NB, USA)] was recorded for 20 min to estimate net photosynthesis (P_{net}), after which the temperature was either increased or decreased to the next target temperature (heat or

cold ramp, respectively). The specifics of collection and analysis of the R, F_v/F_m and P_{net} measurements are detailed below.

The irradiance used here was chosen based on both a photosynthesis–irradiance (P versus E) experiment (Fig. S2), as well as previous photosynthesis experiments on RI *A. poculata* (Jacques et al., 1983). Here, P_{net} was measured at the holding temperature of 18°C at eight light intensities between 5 and 845 µmol photons m^{-2} s^{-1} in four VA-brown individuals. Gross photosynthesis (P_{gross}) of each individual at each light intensity was calculated by subtracting dark respiration (R) measured at 18°C from P_{net}. Using the CFTOOL in MATLAB (vR2016b), the least-squares best fit was calculated for irradiance and P_{gross} for the exponential equation (Fig. S2). An irradiance of 400 µmol photons m^{-2} s^{-1} was chosen for the ramp experiments because it elicited the maximum photosynthesis rate (P_{max}), was well below light levels that induced photoinhibition (Fig. S2), and agreed with previous findings of Jacques et al. (1983). Because the P versus E experiment was conducted at only one temperature (18°C), temperature dependence of the irradiance required to achieve P_{max} was not examined.

The sequence of dark acclimation, R, F_v/F_m, P_{net} and temperature change was repeated at five temperatures for both the heat (18, 22, 26, 29 and 32°C) and cold (18, 15, 12, 9 and 6°C) ramp experiments. A custom-programmed Arduino® MEGA 2560 REV3 (Arduino AG, Somerville, MA, USA) was used to control the water temperature during the ramp experiments (code assembled by D.J.B.). During P, R and F_v/F_m measurements, water temperature was controlled within ±0.5°C of the set temperature. Water temperature was monitored throughout each ramp experiment with a Hobo Pendant® Temperature Data Logger (Onset Computer Corporation; Fig. S1). Once all measurements were completed at the final temperature of each ramp experiment, the fragments were photographed, immediately frozen in liquid nitrogen, wrapped in aluminum foil and stored at −80°C.

Trait measurements
Respirometry
Metabolic rates (R and P_{net}) were determined by measuring changes in dissolved oxygen (O_2) concentration using a fiber-optic O_2 sensor connected to a 10-channel Fiber Optic Oxygen Transmitter (OXY-10 mini, Pre-Sens Precision Sensing GmbH, Regensburg, Germany) in a custom-made acrylic nine-chamber respirometry system. Individual chamber volume was ∼125 ml. The OXY-10 mini instrument was calibrated in accordance with the supplier's manual. Each of the nine chambers was mounted in a Plexiglas base, submerged in a recirculating water bath in the experimental aquarium, positioned on a submersible magnetic stir plate, and a magnetic stir bar was used to maintain constant and turbulent water flow throughout the measurements. Oxygen flux was recorded in a blank chamber (no coral fragment) during each measurement, and this blank metabolic rate was subtracted from the rate calculated in the experimental chambers at the corresponding temperature and measurement to correct for any metabolic activity of microbes in the water or instrument drift.

Oxygen concentrations were recorded using the Pre-Sens software (version Oxy10v3_33fb) at 0.07 Hz and corrected for temperature and salinity of the water based on the correction spreadsheet provided by Pre-Sens. Metabolic rates were calculated from these corrected O_2 concentrations using the LoLinR package (Olito et al., 2017) in R v3.4.0 (https://www.r-project.org/). This package utilizes local linear regression techniques to estimate metabolic rates from time series data in a robust and reproducible way (Olito et al., 2017). Following correction of the O_2 concentrations and calculation of the raw metabolic rate, the metabolic rate for each fragment was normalized

to surface area of the corresponding coral fragment (*sensu* Hoogenboom et al., 2006; Jacques et al., 1983; Lyndby et al., 2018preprint) and corrected for drift. All metabolic rates are expressed in units of μmol O_2 cm^{-2} h^{-1}. P_{gross}, the amount of oxygen produced in the light after accounting for respiratory demands, was calculated by subtracting dark respiration (R) from P_{net}.

Holobiont
Each coral fragment was photographed before and immediately upon completion of each ramp experiment. These photos were used to quantify surface area of each experimental fragment, which was estimated using the image analysis software ImageJ (Schindelin et al., 2015). This 2-D analysis was found to produce a reasonable measure of *A. poculata* surface area, as the majority of colonies collected for this experiment were encrusting, and during fragmentation corals were cut into pieces as uniform in height as possible. These surface area measurements were also used to correct metabolic rates, as described above.

Breviolum psygmophilum photochemical efficiency
In order to quantify *B. psygmophilum* performance throughout the ramp experiments, F_v/F_m was measured in triplicate for each experimental fragment at each temperature of all ramp experiments using a pulse-amplitude modulation fluorometer (JUNIOR-PAM; Heinz Walz GmbH, Effeltrich, Germany) following at least 40 min of dark acclimation. Dark-acclimated F_v/F_m should decrease if the symbionts become thermally stressed (Falkowski and Raven, 2007; Fitt et al., 2001; Thornhill et al., 2008; Warner et al., 1996).

To rule out the effect of time spent in the chamber on *B. psygmophilum* performance, a pilot study was conducted before the ramp experiments during which F_v/F_m was measured six times over the course of 5 h while the coral fragments were held constant at 18°C using the same methods described above (Fig. S4B). Three VA-brown and three VA-white coral fragments were used for this pilot study (different genets than those used for the ramp experiments), and F_v/F_m was measured in triplicate for each individual every hour between 10:00 and 15:00 h.

The same photos described above were also used to approximate chlorophyll and *B. psygmophilum* densities of each fragment following the protocol presented by Winters et al. (2009). Briefly, using the MATLAB macro 'AnalyzeIntensity', mean red channel intensity was calculated for 20 quadrats of 25×25 pixels for each fragment and used as a measure of brightness (i.e. higher brightness indicates fewer algal pigments).

Aquaria conditions
Before each ramp experiment, all experimental corals were maintained in a 325-gallon common garden aquarium with artificial seawater mixed to a salinity of 35 (PSS-78) using Crystal Sea® Bioassay salt (Marine Enterprises International, Baltimore, MD, USA) and deionized water. Temperature was maintained at 18 ±0.5°C using an AquaLogic® temperature controller (AquaLogic, San Diego, CA, USA) in combination with an in-line water chiller (Delta Star®, AquaLogic) and 1500 W SmartOne® Max Bottom immersion heater (Process Technology, Willoughby, OH, USA). The common garden aquarium was equipped with a filter sock for mechanical filtration, protein skimmer for removal of organic material, and powerheads (Tunze® Turbelle, Penzburg, Germany) to maintain flow.

The respirometry experiments were run in a separate experimental aquarium equipped with the custom metabolic chamber set-up previously described. As in the common garden aquarium, artificial

seawater was mixed to 35 (PSS-78) using Crystal Sea® Bioassay salt. Temperature was manipulated using a custom-programmed Arduino® MEGA 2560 REV3 (code assembled by D.J.B.) connected to the same style heater and chiller as the common garden aquarium.

Routine maintenance of *A. poculata* before the ramp experiments included feeding 3 times per week with freshly hatched brine shrimp (*Artemia* sp.), which were distributed over the surface of each fragment using a Pasteur pipette. However, before respirometry experiments, corals were starved for 24 h to standardize metabolic response during ramps. Additionally, weekly water changes of 15% in the common garden aquarium and 100% in the experimental aquarium were performed. Temperature and salinity were monitored daily in both aquaria using an NIST-calibrated thermometer and a refractometer, respectively. Additional nutrient parameters, including nitrate, nitrite, ammonium, phosphate, calcium and magnesium, were monitored bi-weekly using API test kits (Mars Fishcare North America Inc., Chalfont, PA, USA).

Symbiodiniaceae genotyping
Genomic DNA was isolated from n=10 VA and n=10 RI brown individuals following a CTAB-chloroform extraction protocol (Baker and Cunning, 2016) and quantified using a Nanodrop 2000 Spectrophotometer (Thermo Scientific, Waltham, MA, USA). The internal transcribed spacer region 2 (ITS2) was amplified using custom primers incorporating Symbiodiniaceae specific ITS-2-dino-forward and its2rev2-reverse regions (as described in Baumann et al., 2017) and the following PCR profile: 95°C for 5 min, followed by 35 cycles of 95°C for 40 s, 59°C for 2 min, 72°C for 30 s and a final extension of 7 min at 72°C. Each 20 μl reaction contained 2 μl DNA template, 7.8 μl Milli-Q H_2O, 10 μl of 2X BioMix™ Red (Bioline USA, Taunton, MA, USA), and 1 μmol l^{-1} forward and 1 μmol l^{-1} reverse primers. The PCR products were cleaned using the ExoSAP-IT PCR Product Cleanup Kit according to the manufacturer's instructions (Affymetrix Inc., Santa Clara, CA, USA) before a second set of PCRs, which incorporated sequence primers and unique barcodes to each sample using Illumina's Nextera XT Adapter Kit (Illumina, San Diego, CA, USA) *sensu* Kenkel et al. (2013). Samples were pooled and sequenced using a 250 bp paired-end MiSeq Nano Reagent Kit version 2 (Illumina) on ODU's Illumina MiSeq.

Raw reads were de-multiplexed, and counts of distinct operational taxonomic units (OTUs) as well as sequence variants were identified using the DADA2 pipeline (Callahan et al., 2016) in R v3.4.0 (https://www.r-project.org/). Four unique OTUs represented across five individuals (three VA-brown and two RI-brown) passed the filtering steps of DADA2. The representative species of each of the four OTUs was determined by a BLASTn search against the GenBank (NCBI) nucleotide reference collection (nt). The individuals used in this genotyping analysis were not the same as those used in the acute temperature ramp experiments described above. However, they were collected from the same sites in the same year and are therefore considered representative of Symbiodiniaceae communities hosted by *A. poculata* at the particular VA and RI sites discussed here.

Statistical analyses
All statistical analyses were implemented in the R v3.4.0 statistical environment (https://www.r-project.org/). *Astrangia poculata* metabolic rates (R_{corr} and P_{gross}) were analyzed using two approaches. First, holobiont, skeleton and corrected metabolic rates were compared among temperature, symbiotic status and origin using a repeated-measures ANOVA, with fixed factors of temperature, symbiotic status and origin, and genotype included as

the repeated-measure term to account for natural variation between genotype and temperature. When main effects were detected, Tukey's honestly significant difference (HSD) *post hoc* analyses were used to identify significant paired contrasts as indicated in the text. The ANOVA results for R_{corr} and P_{gross} are included in Tables 1 and 2, respectively, and the summaries of all other statistical analyses are included in the electronic notebook associated with this publication (GitHub: https://github.com/BarshisLab/AstrangiaPoculata-Thermal-Performance; figshare: https://doi.org/10.6084/m9.figshare.7619378. v1). Data from both heat and cold ramps were combined for this analysis, after randomly sampling half of the 18°C measurements in order to maintain the same sample size for each temperature.

Second, the entire TPC of each individual was ln transformed and fitted to the Sharpe–Schoolfield equation (Schoolfield et al., 1981) in order to quantify the thermal optimum (T_{opt}) for each individual. The best fit to each TPC was determined by nonlinear least squares regression using the R package nls.multstart (https://CRAN. R-project.org/package=nls.multstart). The Sharpe–Schoolfield equation yields the maximum metabolic rate at T_{opt} (Padfield et al., 2016), which was estimated for each individual. The uncertainty in the Sharpe–Schoolfield fit and parameters, including T_{opt}, was estimated using parametric bootstrapping following the approach outlined by Thomas et al. (2012). This approach was found to be most appropriate for this dataset because the TPCs measured here did not capture many points past T_{opt}. T_{opt} was compared between origin and symbiotic state using a fixed-effects ANOVA, with fixed effects of origin and color. Because we were unable to measure many points past the T_{opt} of the populations, it was difficult to confidently estimate T_{opt} for every individual; therefore, outliers (estimates of $T_{opt}<0$) were excluded from the analysis.

F_v/F_m was analyzed as above, using a repeated-measures ANOVA with fixed factors of temperature, symbiotic status and origin, a repeated-measure term of genotype, and where indicated in text, Tukey's HSD *post hoc* analyses when main effects were detected. The three replicate measurements per individual at each temperature were averaged before analysis and heat and cold ramps were combined with random sampling of half of the 18°C measurements. Holobiont and skeleton F_v/F_m were analyzed separately.

The effects of *A. poculata* origin and color on red channel intensity (i.e. proxy of algal pigments) of the photographs were assessed using a fixed-effects ANOVA, with origin and color included as fixed effects. This analysis was conducted separately for both holobiont and skeleton photos.

The R package MCMCglmm (Hadfield, 2010) was used to calculate the genetic variance–covariance matrices (**G** matrices) separately for VA and RI populations, as well as for both populations combined. For all **G** matrices, trait data were mean-centered and a multivariate model was fit for four traits (R_{corr}, P_{gross},

F_v/F_m and coral color) including data from only 'current conditions' (18 and 22°C). VA and RI population models were fit with temperature as a fixed effect and genotype as a random effect. For the model with both locations included, the multi-trait model included interactive fixed effects of temperature and origin and a random effect of genotype. All three models were run for 25,000 iterations after a 10,000 iteration burn-in, and the Markov chain was stored after 20 iteration intervals. Trait associations were determined to be significant if the 95% credible interval (95% CI) did not include zero. The similarity of the VA and RI **G** matrices was determined by calculating the correlation between them using the random skewers method in the R package EvolQG (Cheverud and Marroig, 2007; Melo et al., 2015). This method utilizes the Lande equation (Lande, 1979) and produces a mean correlation between responses of **G** matrices to the same selective pressure, which is a statistic of how often those populations respond similarly to the same selection pressure (Melo et al., 2015).

RESULTS
In situ thermal environment
Overall, VA SST was greater than RI SST as recorded by the two NOAA buoys over the time course considered here (mean± 1 s.d.=16.8±7.0°C in VA and 12.2±6.7°C in RI; two-sample Kolmogorov–Smirnov test $D=0.299$, $P<0.0002$; Fig. 2A). At the depth of the collection sites, this pattern was maintained for most of the time recorded (Fig. 2A). However, while RI was consistently colder than VA in the winter months, RI was warmer than VA during the summer months (June–August mean±1 s.d.=16.8±3.2°C in VA and 17.8±1.9°C in RI; Fig. 2A, Hobo loggers). This is likely due to the shallower depth of collection of RI corals and therefore a greater amount of time spent above the summer thermocline. The RI site spent 19.2% of the time recorded by *in situ* loggers at the coldest temperatures overall (between 2 and 6°C; Fig. 2B), and the coldest temperature recorded was 3.1°C (14 February 2017 at 04:40 h). In contrast, the coldest temperature recorded by *in situ* loggers in VA was 7.2°C (25 January 2017 at 03:15 h). The VA site spent 17.7% of the time recorded at the warmest temperatures (between 22 and 26°C), whereas the RI site spent only 0.1% of the time recorded between these same temperatures (Fig. 2B). The maximum temperatures recorded by *in situ* loggers at the VA and RI collection sites were 25.0°C (3 September 2016 at 12:15 h) and 23.2°C (28 August 2016 at 15:32 h), respectively.

Metabolic thermal response
We predicted that VA *A. poculata* would maintain higher metabolic rates at greater temperatures (i.e. higher T_{opt}) than RI corals, and vice versa at cold temperatures, owing to adaptation to distinct local thermal environments. Corrected dark respiration (R_{corr}) was

Table 1. Corrected dark respiration (R_{corr}) ANOVA summary for the model R_{corr}~Origin×Color×Temperature+Error (Genotype/Temperature)

Factor	d.f.	SS	MS	F	Pr(>F)
Between subjects					
Origin	1	1.56	1.56	6.36	**0.018**
Color	1	1.50	1.50	6.12	**0.020**
Origin×Color	1	0.0240	0.0244	0.099	0.75
Residuals	28	6.88	0.0246		
Within subjects					
Temperature	1	22.8	22.8	169.2	**<0.0001**
Origin×Temperature	1	0.080	0.080	0.594	0.45
Color×Temperature	1	0.35	0.35	2.59	0.12
Origin×Color×Temperature	1	0.008	0.008	0.058	0.81
Residuals	28	3.78	0.135		

Table 2. Holobiont gross photosynthesis (P_{gross}) ANOVA summary for the model: P_{gross}~Origin×Color×Temperature+Error (Genotype/Temperature)

Factor	d.f.	SS	MS	F	Pr(>F)
Between subjects					
Origin	1	0.61	0.61	3.46	0.073
Color	1	7.57	7.57	42.96	**<0.0001**
Origin×Color	1	0.26	0.26	1.45	0.24
Residuals	28	4.93	0.18		
Within subjects					
Temperature	1	4.64	4.64	21.6	**<0.0001**
Origin×Temperature	1	0.11	0.11	0.489	0.49
Color×Temperature	1	1.75	1.75	8.17	**0.008**
Origin×Color×Temperature	1	0	0	0.001	0.98
Residuals	28	6.001	0.22		

different based on origin ($P=0.02$; Table 1), with RI R_{corr} greater than VA R_{corr} overall (Tukey's HSD, $P=0.003$; Fig. 3). R_{corr} was 1.15 to 1.63 times greater in RI corals compared with VA corals and was different across the majority of the temperatures measured here (Tukey's test of origin×temp: 6°C, $P=0.02$; 15°C, $P=0.03$; 18°C, $P=0.008$; 22°C, $P<0.0001$; and 26°C, $P=0.0002$; Fig. 3), but not at the warmest temperatures measured (29°C and 32°C; Fig. 3). As predicted by Arrhenius kinetics (Angilletta, 2009; Schulte et al., 2011), R_{corr} was affected by temperature ($P<0.0001$; Table 1), and generally increased in both populations up until T_{opt}. R_{corr} of white corals was greater than brown corals overall ($P=0.02$; Fig. 3; Tukey's HSD, $P=0.001$; Table 1) and R_{corr} of RI-white corals was greater than VA-white (Tukey's HSD, $P=0.007$), but not brown corals (Tukey's HSD, $P=0.12$). Additionally, *A. poculata* skeleton dark respiration rates were affected by temperature only but were not different between sites ($P<0.0001$; Fig. S3C).

In contrast to R_{corr}, there was no effect of origin on *A. poculata* holobiont gross photosynthesis (P_{gross}; $P=0.073$; Fig. 4). Holobiont

P_{gross} was higher in brown than in white corals overall ($P<0.0001$; Fig. 4; Tukey's HSD, $P<0.001$; Table 2). P_{gross} was also generally greater at higher temperatures ($P<0.0001$; Table 2). There were interactive effects of color and temperature on P_{gross} ($P=0.008$; Table 2). Within temperatures, P_{gross} was greater in brown than in white corals at all temperatures except 9°C (Fig. 4), which was to be expected based on the holobiont energy budget (i.e. brown corals host photosynthetic symbionts). Despite maintaining rates greater than white colonies, rates of P_{gross} in brown corals overall were low, and indeed the 95% confidence intervals of brown P_{gross} overlapped with 0 μmol O_2 cm^2 h^{-1} at the majority of temperatures for RI (6, 9, 12, 15 and 18°C) and two temperatures for VA (9 and 12°C) corals.

Holobiont P_{gross} is presented here because many of the skeleton O_2 flux measurements in the light were negative (i.e. higher rate of O_2 consumption in the light than in the dark; Fig. S3A) and therefore did not produce a reasonable measure of P_{corr} (Fig. S3B). P_{corr} was affected by color ($P<0.0001$), temperature ($P=0.003$) and the interaction of the two ($P<0.02$). As with dark respiration, skeleton P_{gross} was affected by temperature only ($P=0.01$).

Optimum temperature differs between VA and RI
Individuals with negative estimates of T_{opt} ($n=1$ each for VA-brown, VA-white and RI-brown corals) and two individuals for which T_{opt} could not be estimated (both RI-white corals) were removed from the analysis. Considering only the individuals for which a reasonable (using the above criteria) estimate was obtained ($n=7$ VA-brown, VA-white and RI-brown, and $n=6$ VA-white), the mean±s.d. T_{opt} of each population was 26.8±3.7°C for VA-brown, 28.2±2.7°C for VA-white, 23.0±5.2°C for RI-brown and 21.3±7.9°C RI-white. Within a population, the range in genet T_{opt} was greater in RI corals (RI-brown range=16.3 to 29.0°C; RI-white range=10.2 to 30.1°C) compared with VA corals (VA-brown range=21.7 to 30.2°C; VA-white range=23.2 to 30.7°C; Fig. 3). T_{opt} was higher in VA than in RI corals ($P=0.0134$; Tukey's HSD,
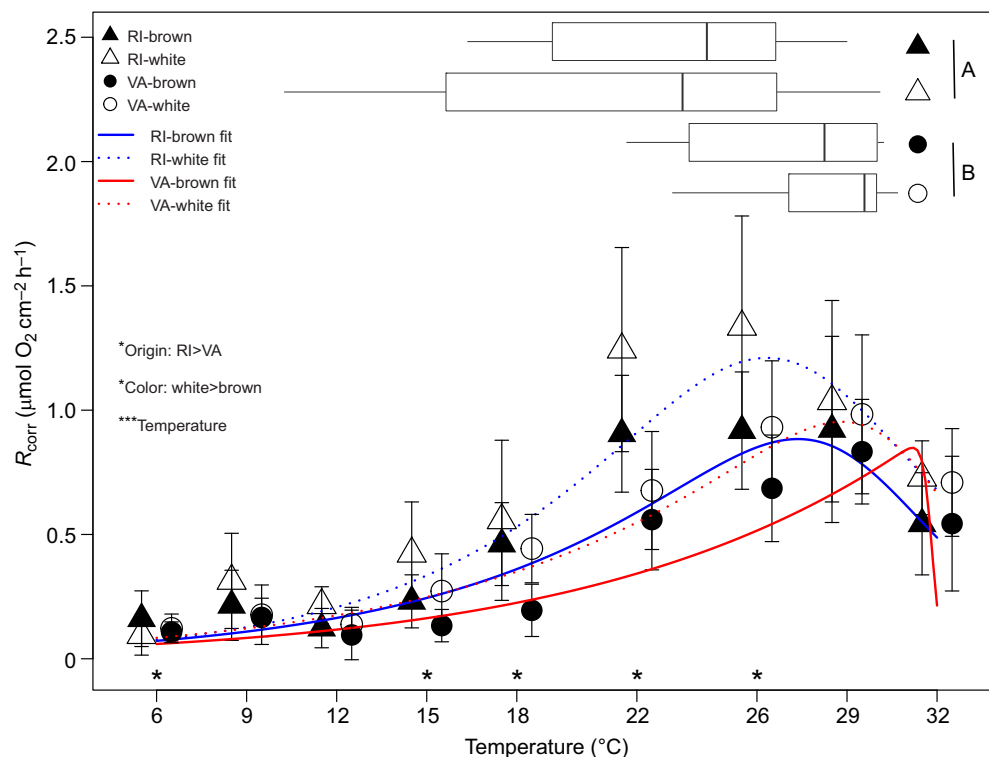

Fig. 3. *Astrangia poculata* corrected dark respiration (R_{corr}) thermal performance curve (TPC) and estimated thermal optimum (T_{opt}). TPCs of dark respiration rates of brown (dark symbols) and white (open symbols) RI (triangles) and VA (circles) corals corrected for rates of skeleton-associated endolithic organisms between 6 and 32°C and the T_{opt} estimates from the same data (box plots). Fit lines (red=VA, blue=RI; dotted=white, solid=brown) are predictions of R_{corr} based on a parametric bootstrapping approach. Origin, color and temperature had a significant effect on corrected dark respiration rates (*$P<0.05$, ***$P<0.0001$). Asterisks above the x-axis indicate temperatures at which significant ($P<0.05$) within-temperature differences between VA and RI corrected respiration were detected, with RI greater than VA in all cases. A and B designations next to the boxplots indicate significant ($P<0.05$) differences in T_{opt} by origin. Each data point of the TPC is an average of $n=8$ distinct individuals and error bars are 95% confidence intervals.
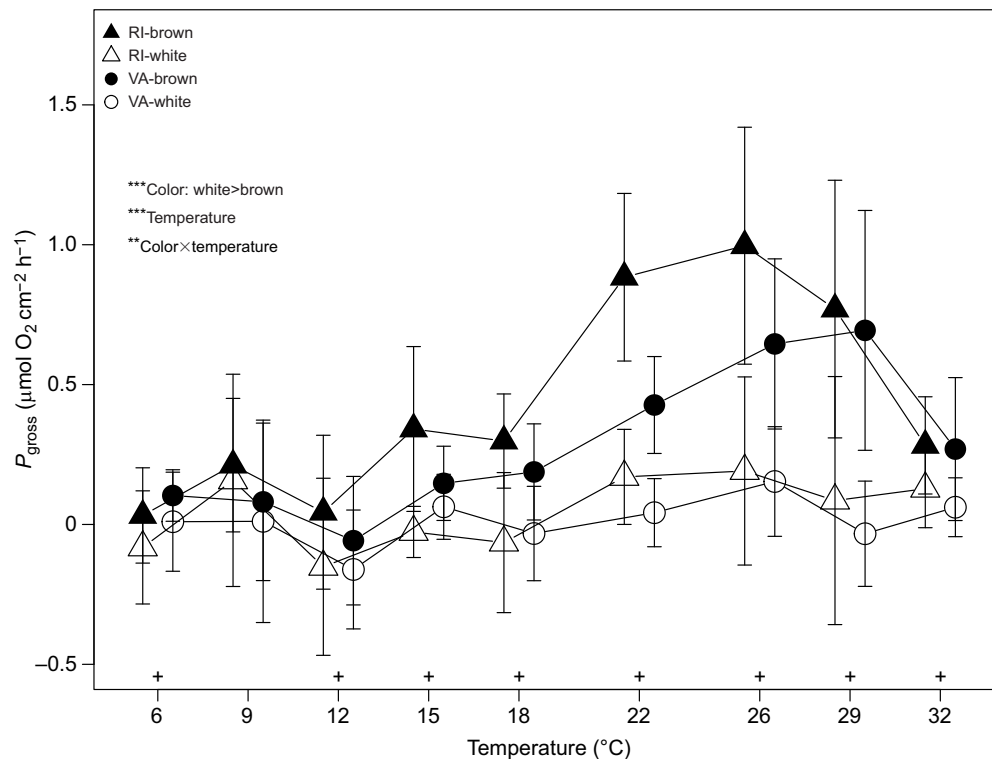
Fig. 4. *Astrangia poculata* holobiont gross photosynthesis. Gross photosynthesis (net photosynthesis – dark respiration) rates of coral holobionts between 6 and 32°C. Color, temperature and color×temperature all had a significant effect on gross photosynthesis rates (**$P<0.01$, ***$P<0.0001$). Plus signs above the x-axis indicate temperatures at which significant ($P<0.05$) within-temperature differences between brown and white gross photosynthesis were detected, with brown greater than white in all cases. Symbols, sample sizes and error bars as denoted in Fig. 3.

$P=0.0125$; Fig. 3), but not different among colors ($P=0.9699$). T_{opt} estimates of the VA population were 3.76°C (brown) and 6.88°C (white) higher than the RI population. Therefore, although RI corals had higher respiration rates than VA corals overall, the VA TPCs were shifted to a higher T_{opt} (Fig. 3).

Effects of temperature on F_v/F_m of *B. psygmophilum*
Temperature affected not only the metabolic rates of *A. poculata*, but also the photochemical efficiency (dark acclimated F_v/F_m) of the symbiont ($P=0.001$; Fig. 5). F_v/F_m was highest at 18°C and different from all other temperatures measured (Tukey's HSD, $P<0.001$) and was greater in brown fragments than in white fragments overall (Tukey's HSD, $P<0.001$). The significant interaction between temperature and symbiotic status ($P=0.001$) is to be expected as aposymbiotic specimens should produce a much attenuated F_v/F_m signal. This pattern was maintained at all temperatures measured except for 32°C, at which point F_v/F_m of brown and white *A. poculata* fragments converged, owing to the higher F_v/F_m of white corals at the warmer temperatures as compared with the cold temperatures (Fig. 5).

F_v/F_m measurements were also different in the coral skeletons, with VA skeleton F_v/F_m lower than that of RI skeleton fragments overall (Tukey's HSD, $P=0.002$; Fig. S4A). Even with the tissue and associated symbionts removed, skeleton F_v/F_m was affected by the original color of the fragment, suggesting the presence of residual photosynthetic tissue in the fragment ($P=0.04$). Lastly, interactive effects of origin and color ($P=0.031$) as well as origin, color and temperature ($P=0.014$) were observed in skeleton F_v/F_m.

The 18°C hold trial experiment revealed an overall effect of time on F_v/F_m ($P=0.0294$). However, there were no differences in F_v/F_m between any of the time points between 10:00 and 15:00 h (Tukey's HSD, $P>0.1$ for all within-time comparisons; Fig. S4B), and the results suggest a possible trend towards increased F_v/F_m over time rather than the decreases seen in the ramp exposures.

Algal pigment concentrations are different between *A. poculata* populations
Analysis of digital photographs taken before beginning the thermal ramp experiments showed that RI holobiont fragments had more algal pigments than VA holobiont fragments (Tukey's HSD, $P=0.003$; Fig. S5A). As expected, holobiont brown corals had more algal pigments than holobiont white corals (Tukey's HSD, $P<0.0001$; Fig. S5A).

As with the holobiont fragments, RI skeleton fragments had greater algal pigment density than VA skeleton fragments (Tukey's HSD, $P<0.001$; Fig. S5B). This pattern was maintained within both brown and white corals (Tukey's HSD, brown: $P=0.0052$, white: $P<0.001$; Fig. S5B).

Genetic architecture of traits does not differ between *A. poculata* populations
The individual VA and RI **G** matrices were positively correlated (vector correlation=0.877, $P=0.03$). Because the **G** matrices are not different between populations, all corals from both locations were combined to make a single **G** matrix to boost confidence in the genetic architecture of these traits (Fig. 6). All trait variance associations were significantly positive (95% CI>0), covariance between P_{gross} and F_v/F_m was significantly positive (95% CI>0), and the covariances between coral color and F_v/F_m, and color and P_{gross} were significantly negative (95% CI<0; Fig. 6).

RI and VA both associate with *B. psygmophilum*
A BLASTn search against the nt database (NCBI) revealed that the four OTUs from the three VA and two RI individuals that passed the filtering steps of the DADA2 analysis (NCBI accession numbers MK024928–MK024930) had at least 99% similarity to *Breviolum psygmophilum* (formerly *Symbiodinium psygmophilum*; strain CCMP2459; NCBI accession number LK934671.1). This species has been previously shown to be the exclusive symbiotic partner of *A. poculata* (LaJeunesse et al., 2012; Thornhill et al., 2008).
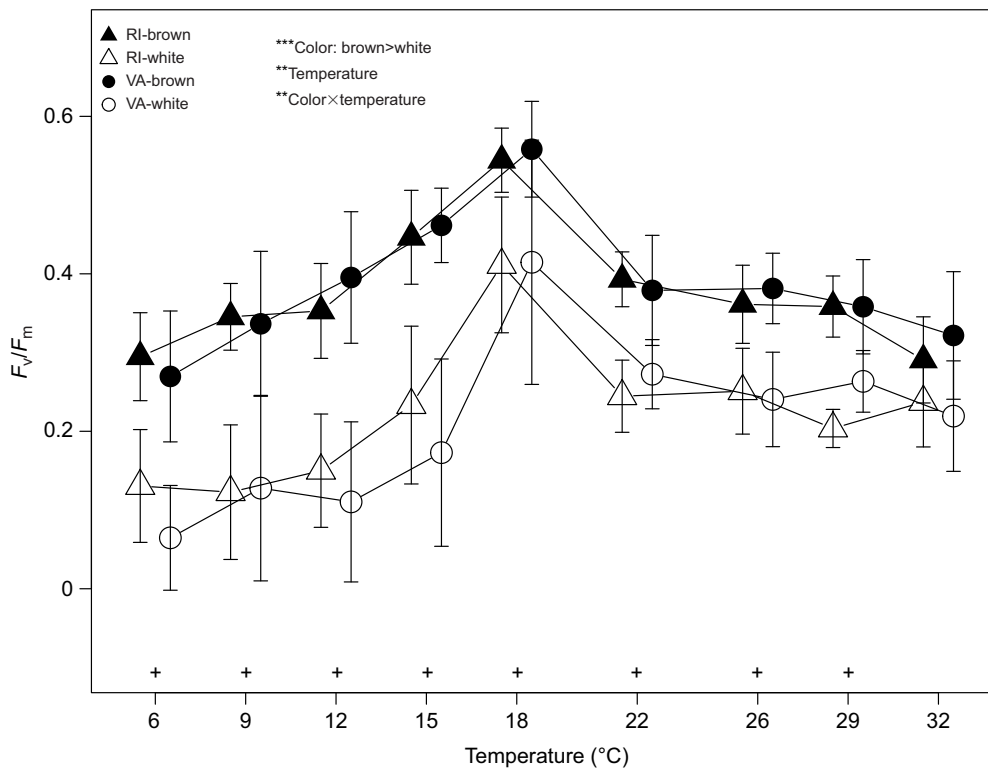
Fig. 5. *Breviolum psygmophilum* photochemical efficiency. Photochemical efficiency of coral holobionts between 6 and 32°C. Color, temperature and color×temperature all had a significant effect on photochemical efficiency (**$P<0.01$, ***$P<0.0001$). Plus signs above the x-axis indicate temperatures at which significant ($P<0.05$) within-temperature differences between brown and white photochemical efficiency were detected, with brown greater than white in all cases. Symbols, sample sizes and error bars as denoted in Fig. 3.

DISCUSSION
Countergradient variation in respiration rate between populations

Adaptation in thermal physiology resulting from environmentally driven selection along a species' range should lead to population-specific differences in thermal performance (Angilletta, 2009). The strongest evidence observed in this study suggesting adaptation to local thermal environments is the consistently higher dark respiration rates (i.e. metabolic activity) exhibited by the RI

Fig. 6. Genetic variance–covariance matrix. Genetic variance–covariance matrix for four fitness traits [gross photosynthesis (P_{gross}), photochemical efficiency [F_v/F_m], coral color and corrected respiration (R_{corr})] across two temperatures (18 and 22°C) and 32 genotypes as calculated using the R package MCMCglmm. The numbers on the diagonal of the matrix are trait variance, and off-diagonal numbers are covariance values between traits. Bold numbers indicate significant trait associations (95% credible interval does not include zero). Lines above the matrix cluster the traits by similarity. Warmer colors indicate more positive variance or covariance.

population across a variety of temperatures. Although the temperature data presented here only span January 2016 through November 2017, the long-term pattern of RI experiencing consistently colder *in situ* temperatures is supported by the NOAA buoy surface temperature data at the sites.

The pattern observed here, in which the cold RI population exhibited higher metabolic rates than the warm VA population across a range of temperatures, is consistent with countergradient variation (Angilletta, 2009; Conover and Schultz, 1995; Gardiner et al., 2010; Sanford and Kelly, 2011), wherein a cold population exhibits an elevated phenotype compared with a warm population at all temperatures. Countergradient variation is one of several patterns that can emerge as a result of adaptive differentiation in a species that inhabits a wide geographic range (Conover et al., 2009; Sanford and Kelly, 2011), and can indicate phenotypic plasticity (Sanford and Kelly, 2011) or fixed genetic differences between the populations (Somero, 2010, 2005). Countergradient variation technically describes populations from distant habitats along the species' range that exhibit similar phenotypes (e.g. respiration rate) in their native environment, and can be identified when the cooler population exhibits an elevated phenotype when acclimated to common garden conditions (Conover and Schultz, 1995; Sanford and Kelly, 2011). Future research should examine metabolic performance of *A. poculata in situ* in RI and VA to further examine whether respiration rates are similar in their native environments compared with the differences in the common garden observed herein.

The metabolic cold adaptation (MCA) hypothesis provides one explanation for countergradient variation, and outlines that populations from colder environments maintain mass-specific metabolic rates greater than counterparts of the same species from warmer regions as an evolutionary adaptation to compensate for lower biochemical reaction rates (Addo-Bediako et al., 2002; Clarke, 1993; Pörtner et al., 1998; Thiel et al., 1996). Pörtner et al. (2000) link the MCA hypothesis to a model of thermal tolerance from an energetic point of view, whereby changes in mitochondrial
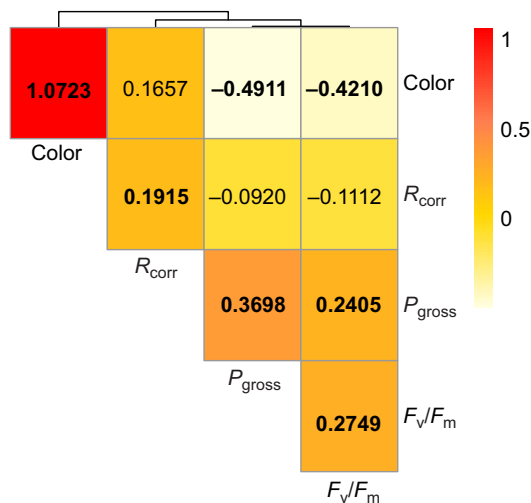
mechanisms may determine an organism's thermal tolerance and lead to differences in base metabolic rates between populations adapted to distinct temperature regimes (Guderley, 2004; Pörtner et al., 1998, 2000; Sommer and Pörtner, 2002). For example, mitochondrial proliferation in a cold-adapted population can promote increased aerobic capacity and a downward shift in the critical thermal minimum (Angilletta, 2009; Pörtner et al., 1998; Sommer and Pörtner, 2002) and result in an elevated baseline metabolic rate (Angilletta, 2009; Pörtner et al., 1998; Sommer and Pörtner, 2002) and a reduced upper thermal limit (Fangue et al., 2009; Pörtner, 2001). Although changes in mitochondrial capacities were not explored here, the hypothesis outlined by Pörtner and colleagues provides one potential explanation for the greater overall dark respiration rates in the RI population of *A. poculata* compared with the VA population as well as the lower T_{opt} of RI corals. In the future, it would be interesting to examine potential differences in mitochondrial density/size in *A. poculata* between RI and VA corals to investigate whether mitochondrial proliferation is driving the enhanced respiration rates of RI corals.

Elevated thermal optima in VA corals

Although population differences in dark respiration were observed, there was no evidence of population differences in R_{corr} at the warmest temperatures measured here (29 and 32°C). This lack of an origin effect at high temperature appears to result from a decline in RI-white coral respiration after 26°C to match rates similar to those of the VA corals. However, we did find evidence of population differences in thermal optima. Although we acknowledge some limitations to these analyses (see below), the estimates of T_{opt} obtained here support our hypothesis and follow the convention of the warmer population (VA) being adapted to its thermal environment and exhibiting a higher thermal optimum (*sensu* Angilletta, 2009). This population difference in T_{opt} is the second line of evidence supporting adaptation to the local thermal environment in VA and RI *A. poculata*, and may indicate a higher upper thermal limit of the VA population.

Because the entire TPC (i.e. the full decline in metabolic rate to the critical thermal maximum) was not captured in these experiments, additional work will be needed to obtain a more confident estimate of T_{opt} for these two populations. Specifically, the experiments described here should be expanded to include temperatures above 32°C to increase confidence in the validity of the T_{opt} estimates. Additionally, this will allow for accurate characterization of other aspects of *A. poculata*'s TPC, such as activation energy (E), thermal breadth and deactivation energy (E_h). However, an important caveat to all of these analyses is that the ability of TPCs to predict performance and fitness (i.e. T_{opt}) can be limited, as reviewed by Sinclair et al. (2016). Nevertheless, the consistent pattern of countergradient variation and elevated T_{opt} observed here are complementary in suggesting real differences in thermal performance between these populations.

Similar photosynthesis and F_v/F_m responses between origins

The adaptive signature observed here appears to be limited to R_{corr} and T_{opt}, as we found no evidence of differences in symbiont performance (P_{gross} or F_v/F_m) or genotype (both hosted *B. psygmophilum*) between VA and RI populations. In addition to the lack of an adaptive signature, rates of *B. psygmophilum* P_{gross} were consistently low (and sometimes negative) in both populations. The negative P_{gross} rates measured here are likely a result of corals performing little measurable photosynthesis (white corals overall, and at some temperatures brown corals), thus

indicating random variation in light and dark respiration and/or lack of instrument sensitivity instead of evidence of light-enhanced respiration (as in Edmunds and Davies, 1988). The negligible rates of P_{gross} measured here suggest that *B. psygmophilum* likely only provides significant photosynthetic by-products (i.e. glucose; Burriesci et al., 2012) to the host at temperatures above 22°C, particularly in RI. This indicates that *A. poculata* likely depends primarily on heterotrophic inputs to meet its metabolic requirements for most of the year. This finding is similar to that of Jacques et al. (1983), who concluded that symbiont photosynthesis was only sufficient to provide a growth benefit to RI *A. poculata* above 15°C, or for 5 to 6 months of the year (also see Dimond and Carrington, 2007).

In terms of photochemical efficiencies, F_v/F_m values of ~0.5 were previously reported in corals collected from the same RI site and maintained at 18°C (Burmester et al., 2017). This supports the convention that the *A. poculata* F_v/F_m measured here at 18°C indicates 'healthy' photochemical efficiency of these populations at this acclimation temperature. However, the significant decreases in F_v/F_m observed at all other temperatures for both VA and RI corals are more difficult to interpret. On the one hand, decreases in F_v/F_m could indicate a stress response of *B. psygmophilum* (Falkowski and Raven, 2007; Fitt et al., 2001). On the other hand, as both RI and VA *A. poculata* regularly experience a range of temperatures in addition to 18°C in the field, it is unlikely that temperatures close to 18°C would induce photochemical stress on *B. psygmophilum in situ*. The 18°C hold pilot study described here provides additional support for this interpretation, as F_v/F_m values did not change over the 5 h the corals were maintained at a constant 18°C. Thus, the pattern observed in the thermal ramp experiments is not likely to be a result of stress associated with time spent in the experimental chambers. Instead, it is more likely that the trend in F_v/F_m with respect to temperature is consistent with acclimation of the photochemical efficiency of *B. psygmophilum* to the common garden aquarium holding conditions.

The experiments conducted here and the facultative symbiosis of *A. poculata* enables the consideration of the influence of Symbiodiniaceae and of the coral host independently. The lack of an effect of origin on the *B. psygmophilum* traits considered here (P_{gross} and F_v/F_m) suggests the coral host may play a larger role in driving the adaptive signature observed in R_{corr} and T_{opt}. The significant effect of origin on R_{corr} within white corals provides additional support for a host-only role in the observed adaptive signature, as these individuals are putatively aposymbiotic and minimally influenced by *B. psygmophilum* physiology.

No population differences in genetic architecture of traits

G matrices are useful in understanding evolutionary potential of a population by considering the geometry of genetic variance and covariance for a set of traits (Aguirre et al., 2014; Steppan et al., 2002). Comparing **G** matrices for multiple populations can determine differences in genetic architecture of traits and how population responses to an identical selective force might differ (Aguirre et al., 2014; Cheverud and Marroig, 2007). Although the structure of the VA and RI **G** matrices were not significantly different from one another, this finding does not diminish our interpretation of the observed pattern of countergradient variation in dark respiration as an adaptive response to local thermal environments. Rather, the similar **G** matrices suggest that the contrasting environment conditions of the two locations may be driving differential selection via similar mechanisms (i.e. on the same traits and via the same pressures but distinguished by differing

environmental conditions). Indeed, phenotypic divergence in the absence of changes in the **G** matrix has previously been observed within ecotypes of an aquatic isopod (*Asellus aquaticus*) from different lakes in Sweden (Eroukhmanoff and Svensson, 2011). Although the genetic architecture of selection mechanisms may not be different between VA and RI *A. poculata*, understanding variation and covariation in traits is valuable in the context of understanding how selection works and how to predict which traits can facilitate or constrain future evolution.

Long-term acclimatization and/or developmental effects

Significant origin effects in a common garden experiment are usually attributed to potential genotypic (i.e. adaptive) effects (DeWitt and Scheiner, 2004; Sanford and Kelly, 2011; Schluter, 2000). However, origin effects are not exclusive of other influences, such as long-term acclimatization and/or developmental/epigenetic drivers. For example, decadal-scale 'environmental memory' was recently observed in the massive coral *Coelastrea aspera* (Brown and Dunne, 2008; Brown et al., 2015). In these studies, former west sides of colonies (experimentally turned to face east) previously exposed to high irradiances bleached less compared with unmanipulated east-facing/low-irradiance sides of colonies despite 10 years of conditioning and identical Symbiodiniaceae phylotypes (Brown and Dunne, 2008; Brown et al., 2015). It is therefore possible that the adaptive signature in dark respiration rates observed here could be attributed to phenotypic plasticity resulting from long-term acclimatization of *A. poculata* to the respective VA and RI thermal environments.

In addition to the effects of long-term acclimatization, the elevated dark respiration rates in RI corals could be the result of persistent maternal effects, developmental canalization and/or epigenetic acclimatization. In order to completely remove the effect of the maternal environment, it would be necessary to rear *A. poculata* for two or more generations under common garden conditions in the laboratory (Sanford and Kelly, 2011; Torda et al., 2017), a process made impractical by both time and resource constraints in this case. As epigenetic mechanisms were not investigated here, we cannot dismiss the possibility that either maternal effects and/or epigenetics played a role in the adaptive signature observed.

Despite these other potential drivers of origin effects, there are several lines of evidence to support a genetic basis behind the adaptive differences and the pattern of countergradient variation in dark respiration rates observed herein. First, previous studies have shown that genetic differentiation can play a significant role in similar patterns of countergradient variation in physiological traits across a latitudinal gradient (Sanford and Kelly, 2011; Somero, 2010, 2005). Second, we did observe a signature of acclimation of photochemical efficiency to common garden conditions (see discussion above), suggesting that the acclimation time was sufficient to remove the effect of the VA and RI thermal environment on *A. poculata*. This conclusion is further supported by Jacques et al.'s (1983) finding that 3 weeks was sufficient to induce physiological acclimation in metabolic rates (specifically respiration) of *A. poculata* coral tissue, similar to the 24-day recovery and acclimation period provided here. Third, the geographic distance separating the two populations considered here supports a pattern of adaptation resulting from reduced gene flow and habitat specialization (Sanford and Kelly, 2011; Wright, 1943). Taken together, this certainly raises the possibility that underlying genetic mechanisms may have led to the observed origin effects on *A. poculata* dark respiration rates.

Conclusions

Patterns of small-scale adaptation are proving to be more ubiquitous in the marine environment than previously believed, which has significant implications when considering population-level responses to environmental change. Here, a consistent pattern of countergradient variation along with elevated thermal optima (T_{opt}) in the warmer VA population compared with the colder RI population suggests a signature of adaptation of VA and RI *A. poculata* to their respective thermal environments. Additionally, the lack of a significant effect of origin on either P_{gross} or F_v/F_m in *B. psygmophilum* along with the origin effect on R_{corr} within white corals suggest a host-only role in the adaptive signature observed here. Although we cannot definitively exclude the contribution of long-term acclimatization, maternal effects and/or epigenetics to the observed effect of origin on dark respiration and T_{opt}, we did observe evidence of acclimation in F_v/F_m to the common garden conditions. This evidence, taken together with previous work demonstrating the acclimation of *A. poculata* metabolic rates over similar timeframes, is suggestive that the significant origin effect observed here could be due to adaptation.

To our knowledge, this study provides the first evidence of adaptation to local thermal environments in the temperate coral *A. poculata*. Although the specific physiological mechanisms that might be under selection along the species' range remain elusive, adaptation of the RI population to the colder thermal environment of the north via mitochondrial proliferation/enlargement could explain the metabolic differences observed here and contribute to the success of this species at its northern range limit.

Author contributions
Conceptualization: H.E.A., R.C.Z., D.J.B.; Methodology: H.E.A., R.C.Z., D.J.B.; Software: H.E.A., D.J.B.; Formal analysis: H.E.A.; Investigation: H.E.A.; Resources: H.E.A., D.J.B.; Data curation: H.E.A.; Writing - original draft: H.E.A.; Writing - review & editing: H.E.A., R.C.Z., D.J.B.; Visualization: H.E.A., D.J.B.; Supervision: D.J.B.; Project administration: D.J.B.; Funding acquisition: H.E.A., D.J.B.

Data availability
DNA sequences have been deposited in NCBI Genbank (accession numbers MK024928–MK024930). All raw data, analyses, scripts, supplementary ANOVA tables and protocols are available as an electronic notebook both on GitHub (https://github.com/BarshisLab/AstrangiaPoculata-Thermal-Performance) and on figshare (https://doi.org/10.6084/m9.figshare.7619378.v1).

Supplementary information
Supplementary information available online at
http://jeb.biologists.org/lookup/doi/10.1242/jeb.189225.supplemental

References

Addo-Bediako, A., Chown, S. L. and Gaston, K. J. (2002). Metabolic cold adaptation in insects: a large-scale perspective. *Funct. Ecol.* **16**, 332-338.

Aguirre, J. D., Hine, E., McGuigan, K. and Blows, M. W. (2014). Comparing G: multivariate analysis of genetic variation in multiple populations. *Heredity* **112**, 21.

Angilletta, M. J. (2009). *Thermal Adaptation: A Theoretical and Empirical Synthesis*. Oxford University Press.

Angilletta, M. J., , Jr, Niewiarowski, P. H. and Navas, C. A. (2002). The evolution of thermal physiology in ectotherms. *J. Therm. Biol.* **27**, 249-268.

Arrhenius, S. (1889). *Über die Dissociationswärme und den Einfluss der Temperatur auf den Dissociationsgrad der Elektrolyte*. Wilhelm Engelmann.

Baker, A. and Cunning, R. (2016). Bulk gDNA extraction from coral samples. *protocols.io.*dyq7vv.

Barshis, D. J., Stillman, J. H., Gates, R. D., Toonen, R. J., Smith, L. W. and Birkeland, C. (2010). Protein expression and genetic structure of the coral *Porites lobata* in an environmentally extreme Samoan back reef: does host genotype limit phenotypic plasticity? *Mol. Ecol.* **19**, 1705-1720.

Barshis, D. J., Birkeland, C., Toonen, R. J., Gates, R. D. and Stillman, J. H. (2018). High-frequency temperature variability mirrors fixed differences in thermal limits of the massive coral *Porites lobata*. *J. Exp. Biol.* **221**, jeb188581.

Baumann, J., Davies, S. W., Aichelman, H. E. and Castillo, K. D. (2017). Coral *Symbiodinium* community composition across the Belize Mesoamerican Barrier Reef System is influenced by host species and thermal variability. *Microb. Ecol.* **75**, 1-13.

Bay, R. A. and Palumbi, S. R. (2014). Multilocus adaptation associated with heat resistance in reef-building corals. *Curr. Biol.* **24**, 2952-2956.

Bay, R. A., Rose, N. H., Logan, C. A. and Palumbi, S. R. (2017). Genomic models predict successful coral adaptation if future ocean warming rates are reduced. *Sci. Adv.* **3**, e1701413.

Brown, B. E. and Dunne, R. P. (2008). Solar radiation modulates bleaching and damage protection in a shallow water coral. *Mar. Ecol. Prog. Ser.* **362**, 99-107.

Brown, B. E., Dunne, R. P., Edwards, A. J., Sweet, M. J. and Phongsuwan, N. (2015). Decadal environmental 'memory' in a reef coral? *Mar. Biol.* **162**, 479-483.

Burmester, E. M., Finnerty, J. R., Kaufman, L. and Rotjan, R. D. (2017). Temperature and symbiosis affect lesion recovery in experimentally wounded, facultatively symbiotic temperate corals. *Mar. Ecol. Prog. Ser.* **570**, 87-99.

Burriesci, M. S., Raab, T. K. and Pringle, J. R. (2012). Evidence that glucose is the major transferred metabolite in dinoflagellate–cnidarian symbiosis. *J. Exp. Biol.* **215**, 3467-3477.

Callahan, B. J., McMurdie, P. J., Rosen, M. J., Han, A. W., Johnson, A. J. A. and Holmes, S. P. (2016). DADA2: high-resolution sample inference from Illumina amplicon data. *Nat. Methods* **13**, 581.

Cheverud, J. M. and Marroig, G. (2007). Comparing covariance matrices: random skewers method compared to the common principal components model. *Genet. Mol. Biol.* **30**, 461-469.

Clarke, A. (1993). Seasonal acclimatization and latitudinal compensation in metabolism: do they exist? *Funct. Ecol.* **7**, 139-149.

Conover, D. O. and Schultz, E. T. (1995). Phenotypic similarity and the evolutionary significance of countergradient variation. *Trends Ecol. Evol.* **10**, 248-252.

Conover, D. O., Duffy, T. A. and Hice, L. A. (2009). The covariance between genetic and environmental influences across ecological gradients. *Ann. N. Y. Acad. Sci.* **1168**, 100-129.

DeFilippo, L., Burmester, E. M., Kaufman, L. and Rotjan, R. D. (2016). Patterns of surface lesion recovery in the Northern Star Coral, *Astrangia poculata*. *J. Exp. Mar. Biol. Ecol.* **481**, 15-24.

DeWitt, T. and Scheiner, S. (2004). Phenotypic variation from single genotypes. In *Phenotypic Plasticity: Functional and Conceptual Approaches* (ed. T. DeWitt and S. Scheiner), pp. 1-9. New York: Oxford University Press.

Dimond, J. and Carrington, E. (2007). Temporal variation in the symbiosis and growth of the temperate scleractinian coral *Astrangia poculata*. *Mar. Ecol. Prog. Ser.* **348**, 161-172.

Edmunds, P. J. and Davies, P. S. (1988). Post-illumination stimulation of respiration rate in the coral *Porites porites*. *Coral Reefs* **7**, 7-9.

Eroukhmanoff, F. and Svensson, E. I. (2011). Evolution and stability of the G-matrix during the colonization of a novel environment. *J. Evol. Biol.* **24**, 1363-1373.

Falkowski, P. G. and Raven, J. A. (2007). *Aquatic Photosynthesis*, 2nd edn. Princeton, NJ: Princeton University Press.

Fangue, N. A., Richards, J. G. and Schulte, P. M. (2009). Do mitochondrial properties explain intraspecific variation in thermal tolerance? *J. Exp. Biol.* **212**, 514-522.

Fitt, W. K., Brown, B. E., Warner, M. E. and Dunne, R. P. (2001). Coral bleaching: interpretation of thermal tolerance limits and thermal thresholds in tropical corals. *Coral Reefs* **20**, 51-65.

García-Ramos, G. and Kirkpatrick, M. (1997). Genetic models of adaptation and gene flow in peripheral populations. *Evolution* **51**, 21-28.

Gardiner, N. M., Munday, P. L. and Nilsson, G. E. (2010). Counter-gradient variation in respiratory performance of coral reef fishes at elevated temperatures. *PLoS ONE* **5**, e13299.

Guderley, H. (2004). Metabolic responses to low temperature in fish muscle. *Biol. Rev.* **79**, 409-427.

Hadfield, J. D. (2010). MCMC methods for multi-response generalized linear mixed models: the MCMCglmm R package. *J. Stat. Softw.* **33**, 1-22.

Hendry, A. P., Taylor, E. B. and McPhail, J. D. (2002). Adaptive divergence and the balance between selection and gene flow: lake and stream stickleback in the Misty system. *Evolution* **56**, 1199-1216.

Hochachka, P. and Somero, G. (2002). *Biochemical Adaptation: Mechanism and Process in Physiological Evolution*. New York: Oxford University Press.

Holcomb, M., McCorkle, D. C. and Cohen, A. L. (2010). Long-term effects of nutrient and CO_2 enrichment on the temperate coral *Astrangia poculata* (Ellis and Solander, 1786). *J. Exp. Mar. Biol. Ecol.* **386**, 27-33.

Holcomb, M., Cohen, A. L. and McCorkle, D. C. (2012). An investigation of the calcification response of the scleractinian coral *Astrangia poculata* to elevated pCO_2 and the effects of nutrients, zooxanthellae and gender. *Biogeosciences* **9**, 29-39.

Hoogenboom, M. O., Anthony, K. R. N. and Connolly, S. R. (2006). Energetic cost of photoinhibition in corals. *Mar. Ecol. Prog. Ser.* **313**, 1-12.

Huey, R. B. and Kingsolver, J. G. (1989). Evolution of thermal sensitivity of ectotherm performance. *Trends Ecol. Evol.* **4**, 131-135.

Huey, R. B. and Kingsolver, J. G. (1993). Evolution of resistance to high temperature in ectotherms. *Am. Nat.* **142**, S21-S46.

Huey, R. B. and Stevenson, R. (1979). Integrating thermal physiology and ecology of ectotherms: a discussion of approaches. *Am. Zool.* **19**, 357-366.

Jacques, T. G. and Pilson, M. E. Q. (1980). Experimental ecology of the temperate scleractinian coral *Astrangia danae* I. Partition of respiration, photosynthesis, and calcification between host and symbionts. *Mar. Biol.* **60**, 167-178.

Jacques, T. G., Marshall, N. and Pilson, M. E. Q. (1983). Experimental ecology of the temperate scleractinian coral *Astrangia danae* II. Effect of temperature, light intensity and symbiosis with zooxanthellae on metabolic rate and calcification. *Mar. Biol.* **76**, 135-148.

Kawecki, T. J. and Ebert, D. (2004). Conceptual issues in local adaptation. *Ecol. Lett.* **7**, 1225-1241.

Kenkel, C. D., Goodbody-Gringley, G., Caillaud, D., Davies, S. W., Bartels, E. and Matz, M. V. (2013). Evidence for a host role in thermotolerance divergence between populations of the mustard hill coral (*Porites astreoides*) from different reef environments. *Mol. Ecol.* **22**, 4335-4348.

Kleypas, J. A., Thomson, D. M., Castruccio, F. S., Curchitser, E. N., Pinsky, M. and Watson, J. R. (2016). Larval connectivity across temperature gradients and its potential effect on heat tolerance in coral populations. *Glob. Change Biol.* **22**, 3539-3549.

LaJeunesse, T. C., Parkinson, J. E. and Reimer, J. D. (2012). A genetics-based description of *Symbiodinium minutum* sp. nov. and *S. psygmophilum* sp. nov. (Dinophyceae), two dinoflagellates symbiotic with Cnidaria. *J. Phycol.* **48**, 1380-1391.

Lande, R. (1979). Quantitative genetic analysis of multivariate evolution, applied to brain: body size allometry. *Evolution* **33**, 402-416.

Lewis, E. (1980). The practical salinity scale 1978 and its antecedents. *IEEE J. Ocean. Eng.* **5**, 3-8.

Loya, Y., Sakai, K., Yamazato, K., Nakano, Y., Sambali, H. and van Woesik, R. (2001). Coral bleaching: the winners and the losers. *Ecol. Lett.* **4**, 122-131.

Lyndby, N., Holm, J. B., Wangpraseurt, D., Grover, R., Rottier, C., Kühl, M. and Ferrier-Pagès, C. (2018). Effect of feeding and thermal stress on photosynthesis, respiration and the carbon budget of the scleractinian coral *Pocillopora damicornis*. *bioRxiv*, 378059.

Matz, M. V., Treml, E. A., Aglyamova, G. V. and Bay, L. K. (2018). Potential and limits for rapid genetic adaptation to warming in a Great Barrier Reef coral. *PLoS Genet.* **14**, e1007220.

Melo, D., Garcia, G., Hubbe, A., Assis, A. P. and Marroig, G. (2015). EvolQG-An R package for evolutionary quantitative genetics. *F1000Research* **4**.

Olito, C., White, C. R., Marshall, D. J. and Barneche, D. R. (2017). Estimating monotonic rates from biological data using local linear regression. *J. Exp. Biol.* **220**, 759-764.

Padfield, D., Yvon-Durocher, G., Buckling, A., Jennings, S. and Yvon-Durocher, G. (2016). Rapid evolution of metabolic traits explains thermal adaptation in phytoplankton. *Ecol. Lett.* **19**, 133-142.

Palumbi, S. R. (2004). Marine reserves and ocean neighborhoods: the spatial scale of marine populations and their management. *Annu. Rev. Environ. Resour.* **29**, 31-68.

Palumbi, S. R., Barshis, D. J., Traylor-Knowles, N. and Bay, R. A. (2014). Mechanisms of reef coral resistance to future climate change. *Science* **344**, 895-898.

Peters, E. C., Cairns, S. D., Pilson, M. E., Wells, J. W., Jaap, W. C., Lang, J. C., Vasleski, C. and St Pierre Gollahon, L. (1988). Nomenclature and biology of *Astrangia poculata* (=*A. danae*, =*A. astreiformis*) (Cnidaria: Anthozoa). *Proc. Biol. Soc. Wash.* **101**, 234-250.

Pörtner, H. (2001). Climate change and temperature-dependent biogeography: oxygen limitation of thermal tolerance in animals. *Naturwissenschaften* **88**, 137-146.

Pörtner, H.-O., Hardewig, I., Sartoris, F. J. and Van Dijk, P. L. M. (1998). Energetic aspects of cold adaptation: critical temperatures in metabolic, ionic and acid-base regulation. *Cold Ocean Physiol.* **66**, 88-120.

Pörtner, H.-O., Van Dijk, P., Hardewig, I. and Sommer, A. (2000). Levels of metabolic cold adaptation: tradeoffs in eurythermal and stenothermal ectotherms. In *Antarctic Ecosystems: Models for Wider Ecological Understanding* (ed. W. Davison and C. H. Williams), pp. 109-122. Christchurch: Caxton Press.

Rhein, H., Rintoul, S. R., Aoki, S., Campos, E., Chambers, D. and Feely, R. A. (2013). Observations: Ocean. In *Climate Change 2013: The Physical Science* (ed. T. F. Stocker, D. Qin, G.-K. Plattner, M. Tignor, S. K. Allen and J. Boschung), pp. 255-316. Basis Contribution of Working Group I to the Fifth Assessment Report of the IPCC: Cambridge University Press.

Ries, J. B. (2011). A physicochemical framework for interpreting the biological calcification response to CO2-induced ocean acidification. *Geochim. Cosmochim. Acta* **75**, 4053-4064.

Sanford, E. and Kelly, M. W. (2011). Local adaptation in marine invertebrates. *Annu. Rev. Mar. Sci.* **3**, 509-535.

Schindelin, J., Rueden, C. T., Hiner, M. C. and Eliceiri, K. W. (2015). The ImageJ ecosystem: an open platform for biomedical image analysis. *Mol. Reprod. Dev.* **82**, 518-529.

Schluter, D. (2000). *The Ecology of Adaptive Radiation*. Oxford: Oxford University Press.

Schoolfield, R. M., Sharpe, P. J. H. and Magnuson, C. E. (1981). Non-linear regression of biological temperature-dependent rate models based on absolute reaction-rate theory. *J. Theor. Biol.* **88**, 719-731.

Schulte, P. M., Healy, T. M. and Fangue, N. A. (2011). Thermal performance curves, phenotypic plasticity, and the time scales of temperature exposure. *Integr. Comp. Biol.* **51**, 691-702.

Sinclair, B. J., Marshall, K. E., Sewell, M. A., Levesque, D. L., Willett, C. S., Slotsbo, S., Dong, Y., Harley, C. D. G., Marshall, D. J. and Helmuth, B. S. (2016). Can we predict ectotherm responses to climate change using thermal performance curves and body temperatures? *Ecol. Lett.* **19**, 1372-1385.

Somero, G. N. (2005). Linking biogeography to physiology: evolutionary and acclimatory adjustments of thermal limits. *Front. Zool.* **2**, 1.

Somero, G. N. (2010). The physiology of climate change: how potentials for acclimatization and genetic adaptation will determine 'winners' and 'losers'. *J. Exp. Biol.* **213**, 912-920.

Sommer, A. M. and Pörtner, H.-O. (2002). Metabolic cold adaptation in the lugworm *Arenicola marina*: comparison of a North Sea and a White Sea population. *Mar. Ecol. Prog. Ser.* **240**, 171-182.

Steppan, S. J., Phillips, P. C. and Houle, D. (2002). Comparative quantitative genetics: evolution of the G matrix. *Trends Ecol. Evol.* **17**, 320-327.

Tepolt, C. K. and Somero, G. N. (2014). Master of all trades: thermal acclimation and adaptation of cardiac function in a broadly distributed marine invasive species, the European green crab, *Carcinus maenas*. *J. Exp. Biol.* **217**, 1129-1138.

Thiel, H., Pörtner, H.-O. and Arntz, W. (1996). Marine life at low temperatures-a comparison of polar and deep-sea characteristics. In *Deep-sea and Extreme Shallow-water Habitats: Affinities and Adaptations*, Vol. 11 (ed. F. Uiblein, J. Ott and M. Stachowitsch), pp. 183-219. Vienna: Austrian Academy of Sciences.

Thomas, M. K., Kremer, C. T., Klausmeier, C. A. and Litchman, E. (2012). A global pattern of thermal adaptation in marine phytoplankton. *Science* **338**, 1085-1088.

Thornhill, D. J., Kemp, D. W., Bruns, B. U., Fitt, W. K. and Schmidt, G. W. (2008). Correspondence between cold tolerance and temperate biogeography in a Western Atlantic *Symbiodinium* (Dinophyta) lineage. *J. Phycol.* **44**, 1126-1135.

Torda, G., Donelson, J. M., Aranda, M., Barshis, D. J., Bay, L., Berumen, M. L., Bourne, D. G., Cantin, N., Foret, S., Matz, M. et al. (2017). Rapid adaptive responses to climate change in corals. *Nat. Clim. Change.* **7**, 627.

van Woesik, R., Sakai, K., Ganase, A. and Loya, Y. (2011). Revisiting the winners and the losers a decade after coral bleaching. *Mar. Ecol. Prog. Ser.* **434**, 67-76.

Veron, J. E. (2000). *Corals of the World*, Vol. 1-3. Townsville: Australian Institute of Marine Science.

Warner, M. E., Fitt, W. K. and Schmidt, G. W. (1996). The effects of elevated temperature on the photosynthetic efficiency of zooxanthellae in hospite from four different species of reef coral: a novel approach. *Plant Cell Environ.* **19**, 291-299.

Winters, G., Holzman, R., Blekhman, A., Beer, S. and Loya, Y. (2009). Photographic assessment of coral chlorophyll contents: implications for ecophysiological studies and coral monitoring. *J. Exp. Mar. Biol. Ecol.* **380**, 25-35.

Wright, S. (1943). Isolation by distance. *Genetics* **28**, 114-138.